Published in final edited form as:
Neuron. 2006 December 7; 52(5): 883–896.

Spatiotemporal Asymmetry of Associative Synaptic Plasticity in Fear Conditioning Pathways

Ryong-Moon Shin, **Evgeny Tsvetkov**, and **Vadim Y. Bolshakov***
Department of Psychiatry, McLean Hospital, Harvard Medical School 115 Mill Street, Belmont, Massachusetts 02478

Abstract

Input specific long-term potentiation (LTP) in afferent inputs to the amygdala serves an essential function in the acquisition of fear memory. Factors underlying input specificity of synaptic modifications implicated in information transfer in fear conditioning pathways remain unknown. Here we show that the strength of naïve synapses in two auditory inputs converging on a single neuron in the lateral nucleus of the amygdala is only modified when a postsynaptic action potential closely follows a synaptic response. The stronger inhibitory drive in thalamic pathway, as compared to cortical input, hampers the induction of LTP at thalamo-amygdala synapses, contributing to the spatial specificity of LTP in convergent inputs. These results indicate that spike timing-dependent synaptic plasticity in afferent projections to the LA is both temporarily and spatially asymmetric, thus providing a mechanism for the conditioned stimulus discrimination during fear behavior.

Fear conditioning is an experimental model of associative learning that is instrumental to our understanding of how sensory stimuli are encoded and retained as a memory of behavioral experiences (LeDoux, 2000; Davis and Whalen, 2001; Maren and Quirk, 2004; Fanselow and Poulos, 2005). During this form of learning, an innocuous conditioned stimulus (CS) becomes biologically meaningful as a result of its temporal association with an aversive unconditioned stimulus (an electric footshock, US). When the CS-US association is learned, the CS alone triggers fear responses. Initially neutral cues of any sensory modality such as sound, light, smell or touch could become the CS after a few pairings with the US during behavioral training (Maren, 2001). The amygdala complex, composed of several subcortical nuclei, provides the neural substrate for the CS-US association during fear conditioning (LeDoux, 2000; Goosens et al., 2003). Anatomical and functional studies have identified the lateral nucleus of the amygdala (LA) as a site where the signals encoding the CS and US converge (Pitkanen et al., 1997; LeDoux, 2000).

Auditory fear conditioning is particularly well-characterized, both in respect to the implicated neural circuitry and underlying cellular mechanisms (Maren and Quirk, 2004). During this form of learning, information about the characteristics of the CS (audible sound) is delivered to the LA via two different routes, a direct input to the LA originating in the auditory thalamus and an indirect pathway extending from the auditory cortex (LeDoux, 2000; Maren, 2001). It has been recently demonstrated that fear conditioning is associated with persistent synaptic enhancements in auditory inputs to the LA (McKernan and Shinnick-Gallagher, 1997; Rogan et al., 1997). Both associative LTP in the LA and fear conditioning demonstrate an identical sensitivity to stimulus contingency, indicating that they might be governed by similar mechanisms (Bauer et al., 2001). Moreover, behavioral training induces LTP-like enhancements of synaptic transmission in cortico-amygdala pathway that both mimic and

*Correspondence should be addressed to V.Y.B. (vadimb@mclean.harvard.edu)

occlude LTP in slices induced with electrical stimulation, thus providing evidence that LTP in auditory inputs to the LA and fear learning are causally linked (Tvetkov et al., 2002).

Experimental animals that are conditioned to fear specific cues can discriminate between conditioned stimuli of distinct modalities and show no signs of generalization of conditioned responses (Campeau and Davis, 1995). As LTP is a likely cellular mechanism of fear learning, input specificity of LTP in afferent inputs to the LA, observed under physiological conditions (Doyere et al., 2003; Tsvetkov, 2004), could contribute to the stimulus discrimination after the CS-US association is formed. It remains unclear, however, how the information that is contained in the specific afferent input activity could be specifically encoded and preserved during fear learning. We addressed this issue experimentally by studying the properties of spike timing-dependent plasticity at two independent inputs, thalamo-amygdala and cortico-amygdala pathways, which relay to the LA information about different characteristics of the CS during auditory fear conditioning (LeDoux, 2000). Spike timing-dependent plasticity (STDP) at central synapses can be induced by precise temporal associations between presynaptic input and postsynaptic action potentials (Bauer et al., 2001; Bi and Poo, 2001; Sjostrom et al., 2001; Feldman, 2002; Bi and Rubin, 2005). Learning rules based on this recently discovered form of synaptic plasticity drew significant attention due to their apparent computational value (Karmarkar et al., 2002).

We found that synaptic modifications in convergent cortical and thalamic inputs in the LA demonstrate temporal and spatial specificity. The observed spatiotemporal asymmetry of synaptic plasticity in afferent inputs to the LA could contribute to the encoding of the information about the particular CS and, thus, to the CS recognition during retrieval of the conditioned response.

Results

Spike Timing-Dependent LTP in the Cortical and Thalamic Inputs to the LA

To explore how spatial specificity of the information flow might be determined in fear conditioning pathways, we investigated the rules that govern spike-timing LTP in two inputs known to be implicated in the acquisition of fear to auditory stimulation and converging on the same principal neuron in the LA. We recorded glutamatergic excitatory postsynaptic potentials (EPSPs) in neurons in the LA in current-clamp mode at the cortico-amygdala or thalamo-amygdala synapses (Tsvetkov et al., 2002; Shumyatsky et al., 2005). As we have previously demonstrated, these convergent inputs to the LA could be reliably separated with our stimulation technique resulting in activation of independent sets of synapses (Tsvetkov et al., 2004).

Pairing of 80 presynaptic pulses, delivered to the fibers either in the external capsule (cortical input, Figure 1A; also see Supplemental Figure 1A) or the internal capsule (thalamic input, Figure 1E) at a 2 Hz-frequency, with action potentials evoked in the postsynaptic cell with 4-8 ms delay from the onset of each EPSP by short depolarizing current injections through the recording electrode (Humeau et al., 2005; Shumyatsky et al., 2005) led to substantial LTP in both pathways, when γ-aminobutyric acid A receptors ($GABA_AR$) were blocked with a specific antagonist, picrotoxin (100 μM, Figures 1B and 1D; Figures 1F and 1H). Forty minutes after the induction, the EPSP in the cortical input was potentiated to 155% ±9% (n = 12) of its pre-LTP amplitude (t test, $p < 0.01$ vs. baseline). In thalamic pathway, the EPSP was potentiated to 142% ±5% (n = 6; t test, $p < 0.01$ vs. baseline) of the initial value. The difference in the magnitude of LTP between cortico-amygdala and thalamo-amygdala synapses with $GABA_AR$-mediated inhibition blocked was not statistically significant (t test, $p = 0.39$).

We next characterized the requirements for the induction of spike timing-dependent LTP in both cortical and thalamic inputs to the LA. Similar to the conventional rate- and voltage-dependent LTP in the amygdala (Huang and Kandel, 1998; Weisskopf et al., 1999; Tsvetkov et al., 2002), spike timing-dependent LTP in cortico-amygdala and thalamo-amygdala pathways required postsynaptic Ca^{2+} influx and was prevented in either input by the inclusion of a high concentration of the Ca^{2+} chelator BAPTA (10 mM) in the recording pipette solution. This experimental intervention is known both to decrease resting intracellular Ca^{2+} concentration and effectively block postsynaptic Ca^{2+} transients in response to stimulation (Bolshakov and Siegelbaum, 1994). Under these conditions, the EPSP remained at 101% ±4% ($n = 4$; $p = 0.46$ vs. the baseline amplitude; significantly different from control LTP, $p < 0.003$) and 113% ±7% ($n = 10$; $p = 0.61$ vs. the baseline amplitude; significantly different from control LTP, $p < 0.02$) of its initial value in cortical (Figures 1C and 1D) and thalamic (Figures 1G and 1H) inputs, respectively, when measured 35-40 min after the delivery of the LTP-inducing stimulation.

With this induction protocol, LTP was also completely blocked by the N-methyl-D-aspartate receptor (NMDAR) antagonist D-2-amino-5-phosphonopentanoic acid (D-APV, 50 μM), either in cortical or thalamic input. When assessed 35-40 min after the LTP-inducing stimulation, the EPSP amplitude was 99% ±12% ($n = 4$; $p = 0.7$ vs. the baseline; significantly different from control LTP, $p < 0.01$) and 104% ±13% ($n = 6$; $p = 0.74$ vs. the baseline; significantly different from control LTP, $p < 0.03$) of the initial value in cortical (Figures 1C and 1D) and thalamic (Figures 1G and 1H) inputs, respectively. It does not rule out, however, the possibility that calcium influx through voltage gated calcium channels may also contribute to the induction process under certain conditions (Weisskopf et al., 1999;Tsvetkov et al., 2002). Consistent with the role of NMDA receptors in LTP induction (Bauer et al., 2002), we found that spike triggering in the absence of synaptic activation did not result in LTP in either pathway, with the cortico-amygdala EPSP remaining at 102% ±2% of the pre-induction response ($n = 3$; not significantly different from the baseline EPSP, t test, $p = 0.38$), while the thalamo-amygdala EPSP was 104% ±10% ($n = 4$; not significantly different from the baseline EPSP, t test, $p = 0.73$) of the initial amplitude, indicating the need for glutamate release in the induction process. Thus, it appears that similar cellular mechanisms are implicated in the induction of spike timing-dependent LTP at convergent cortical and thalamic inputs to the LA.

LTP Induction in Cortical and Thalamic Inputs to the LA is Under Differential Inhibitory Control

Recent findings indicate that the susceptibility of glutamatergic synapses in the LA to LTP is tightly controlled by GABA-mediated inhibition of the principal neurons (Shumyatsky et al., 2002; Bissiere et al, 2003). Therefore, we examined LTP at the cortico-amygdala or thalamo-amygdala synapses without the $GABA_A$R antagonist picrotoxin in the bath solution. Consistent with a previous report (Bissiere et al., 2003), we found that when $GABA_A$R-mediated inhibition was intact the EPSP-spike induction protocol failed to induce LTP in thalamo-amygdala pathway. Forty minutes after the induction, the thalamo-amygdala EPSP remained at 103% ±6% ($n = 5$) of the initial value (Figures 1F and 1H, not significantly different from the baseline EPSP amplitude, t test, $p = 0.69$). Surprisingly, LTP in cortical input was diminished ($p < 0.03$ versus LTP magnitude when $GABA_A$ receptors were blocked) but still could be observed, with the EPSP potentiated to 126% ±6% ($n = 9$) of the initial value (Figures 1B and 1D, significantly different from the baseline EPSP amplitude, t test, $p < 0.01$). The observed effect of the $GABA_A$R antagonist on LTP implies a differential (input specific) inhibitory control of the induction mechanisms in two convergent inputs in the LA.

Time Window for the Induction of Spike Timing-Dependent Plasticity in the LA is Narrow and Asymmetric

To characterize temporal characteristics of spike timing-dependent plasticity in the LA, we varied the interval between the stimulus-induced EPSP and the peak of the action potential (AP) triggered in the LA neuron (Bi and Poo, 2001), thus extending the above-described LTP experiments (see Figure 1). In agreement with previous studies, we found that the time window for LTP induction in the LA with the EPSP-AP protocol was very narrow, as pairing of presynaptic stimulation with postsynaptic action potentials evoked with delays longer than 10 ms did not induce LTP in either pathway (Figures 2A-2D). As shown in Figure 2B, temporal window for LTP induction with the EPSP-AP pairing protocol (the EPSP precedes spike) in cortico-amygdala pathway did not depend on $GABA_A$R-mediated inhibition. With inhibition blocked, the EPSP-AP timing requirements in thalamic input were identical to those observed at cortical pathway. However, no significant LTP was observed at thalamo-amygdala synapses when inhibition was intact (no PTX) with the EPSP-AP intervals ranging from ~0 to ~30 ms (Figure 2D).

We further studied the principles that underlie spike-timing plasticity in the LA by reversing the temporal order of the pre- and postsynaptic activation. The repetitive AP-EPSP paring (the AP precedes the EPSP) has previously been shown to produce long-term depression (LTD) of glutamatergic responses at several different synapses (Bi and Poo, 2001; Wang et al., 2005). Surprisingly, in our experiments triggering postsynaptic spikes before EPSPs did not result in LTD at naive synapses either in thalamic or cortical input to the LA. LTD was absent both with intact inhibition and under conditions when inhibition was blocked, regardless of the inter-pulse interval in the AP-EPSP pair (Figures 2A-2D).

Thus thirty five minutes after the pairing procedure with the AP-EPSP intervals ranging from ~0 to ~30 ms, the EPSP in cortical input remained at 105% ±3% (n = 12) and 104% ±3% (n = 12) of the baseline amplitude in the presence of picrotoxin (blocked inhibition, Figure 2E, closed symbols; not significantly different from the baseline EPSP, t test, $p = 0.12$) or in the absence of picrotoxin (intact inhibition, Figure 2E, open symbols; not significantly different from the baseline EPSP, t test, $p = 0.25$), respectively. In thalamic pathway, the EPSP remained at 106% ±5% (n = 9) and 104% ±4% (n = 11) of the initial value in the presence (Figure 2F, closed symbols; not significantly different from the baseline EPSP, t test, $p = 0.1$) or in the absence of picrotoxin (Figure 2F, open symbols; not significantly different from the baseline EPSP, t test, $p = 0.19$), respectively. To test whether susceptibility of the studied synapses to spike timing-dependent LTD depends on the frequency of plasticity-inducing stimulation, we varied the frequency at which the AP-EPSP pairs were evoked in both convergent inputs. Repetitive AP-EPSP paring with the AP preceding the EPSP by 5-15 ms did not result in significant LTD at any of the frequencies tested (0.2 Hz, 0.5 Hz, 1 Hz or 2 Hz) either in cortical or thalamic pathway (Figure 2G; $p > 0.05$ for each point in the graph, not significantly different from the baseline EPSP). Thus synapses in afferent inputs to the LA are only modified when postsynaptic AP follows the EPSP with a short delay.

Cortical and Thalamic Inputs Do Not Differ in Quantal Parameters of Glutamatergic Synaptic Transmission

Input-specific differences in spike timing-dependent LTP between convergent pathways, observed when $GABA_A$R-mediated inhibition was intact, could be explained by differential (pathway specific) sensitivity of the induction mechanisms to the identical levels of inhibitory control. According to this notion, detectable distinctions in parameters of glutamatergic synaptic transmission should exist between cortical and thalamic inputs.

To directly compare the parameters of synaptic transmission between cortical and thalamic inputs, we first tested the rate of blockade of the whole-cell NMDAR EPSC by an irreversible blocker of the NMDA receptors, MK-801 (40 μM; Huettner and Bean, 1988). In the presence of MK-801, the rate with which the NMDAR EPSC declines in the course of repetitive presynaptic stimulation is positively correlated with the basal Pr (Hessler et al, 1993). We recorded whole-cell NMDAR EPSCs in the presence of the α-amino-3-hydroxy-5-methyl-4-isoxazolepropionic acid (AMPA) receptor antagonist 6-cyano-7-nitroquinoxaline-2,3-dione (CNQX, 20 μM) at a holding potential of -40 mV to relieve the Mg^{2+} block of NMDAR channels (Figures 3A and 3B). When MK-801 blocking rates were estimated in both convergent pathways, there was no difference between cortical and thalamic inputs to the LA (Figure 3C; cortical input, n = 9; thalamic input, n = 9; no significant difference, ANOVA, p = 0.74).

Second, we obtained quantal size estimates in both cortical and thalamic inputs by measuring the amplitude of asynchronously released single quanta of glutamate when strontium (Sr^{2+}) was substituted for extracellular Ca^{2+} (Oliet et al., 1996). Under these conditions, the synchronous component of evoked neurotransmitter release is significantly diminished, while asynchronous release is enhanced and could be observed for hundreds of milliseconds after the presynaptic stimulus (Xu-Friedman and Regehr, 2000; Figures 3D and 3E). This allowed us to analyze quantal events originating from the specific synaptic inputs. Using this approach, we found that quantal size was very similar in two convergent pathways. Thus, the mean amplitude of asynchronous quantal events recorded in the presence of Sr^{2+} was 15.1 ±1.2 pA (n = 10) and 14.9 ±0.9 pA (n = 12) in cortical and thalamic inputs, respectively (Figures 3F and 3G; no significant difference between two inputs, t test, p = 0.92). These data indicate that cortico-amygdala and thalamo-amygdala synapses do not differ either in their basal Pr or quantal amplitude.

Spatiotemporal Specificity of Spike Timing-Dependent Plasticity in the LA is Not Mediated by Different NMDA Receptor Subtypes

As the induction of spike timing-dependent LTP in the LA requires postsynaptic Ca^{2+} influx through NMDA receptors (see above), we asked whether distinct NMDA receptor subtypes could make differential contribution to the induction of synaptic plasticity in afferent inputs to the LA (see Liu et al., 2004).

Using whole-cell voltage-clamp recordings from pyramidal neurons, we confirmed that both NR2A and NR2B subunit-containing NMDA receptors are functionally expressed at cortico-amygdala and thalamo-amygdala synapses (Lopez de Armenia and Sah, 2003; Figure 4). Addition of the selective NR2B antagonist ifenprodil (10 μM) or the NR2A antagonist NVP-AAM077 (0.5 μM; Liu et al., 2004) to the external solution produced progressive decreases in the amplitude of the isolated NMDAR EPSC recorded at a holding potential of +50 mV in the presence of CNQX either in cortical or thalamic pathway (Figures 4A and 4D). The degree of inhibition was very similar at both convergent inputs, as ifenprodil reduced the magnitude of the NMDAR EPSC by 25.1% ±2% (n = 5) and 22.6% ±6% (n = 5) of its baseline value in cortical and thalamic inputs, respectively (Figures 4B and 4C; no significant difference between inputs, t test, p = 0.71). In the presence of the NR2A antagonist NVP-AAM077, the NMDAR EPSC was reduced by 72.2% ±2% (n = 8) and 65.5% ±5% (n = 7) of its baseline value in cortical and thalamic inputs, respectively (Figures 4E and 4F; no significant difference between inputs, t test, p = 0.24).

Despite the fact that NMDA receptor responses were largely mediated by the NR2A containing receptors, the blockade of NR2B subunit abolished spike timing-dependent LTP in both inputs to the LA, while NR2A antagonist had no effect. Thus in the presence of ifenprodil (10 μM, NR2B antagonist), 35 - 40 minutes after the LTP-inducing stimulation the EPSP remained at 105.4% ±8% (n = 9; p = 0. 48 vs. the baseline amplitude; significantly different from control

LTP as shown in Figure 5A, $p < 0.02$) and 107.7% ±16% ($n = 5$; $p = 0.85$ vs. the baseline amplitude; significantly different from control LTP as shown in Figure 5B, $p < 0.04$) of its initial value in cortical (Figures 5B and 5C) and thalamic (Figures 5E and 5F) inputs, respectively. With the NR2A antagonist NVP-AAM077 in the bath solution, the EPSP was potentiated to 128.9 ±12% ($n = 6$, $p < 0.05$ vs. the baseline amplitude) and 141.1 ±8% ($n = 6$, $p < 0.02$ vs. the baseline amplitude) in cortical (Figures 5B and 5C; not significantly different from control LTP, t test, $p = 0.47$) and thalamic inputs (Figures 5E and 5F; not significantly different from control LTP, t test, $p = 0.85$), respectively.

It has been recently demonstrated that NVP-AAM077, at a concentration used in our study, nearly completely blocked NR2A-containing receptors, while a significant fraction of the current mediated by NR2B-containing receptors still remained intact (Neyton and Paoletti, 2006). We found that despite an approximately 70% block of the integral NMDAR current, NVP-AAM077 (500 nM) had no effect on spike timing-dependent LTP at amygdala synapses. The remaining NR1/NR2B receptor-mediated current, though partially blocked by NVP-AAM077, apparently is sufficient to support LTP induction. Based on this observation we can exclude the role of NR2A-containing receptors in the induction process.

These results suggest that subunit composition of synaptic NMDA receptors in cortical input is not different from that in thalamic pathway, and that activation of synaptic NR2B-containing NMDA receptors accounts for the induction of spike timing-dependent LTP at both convergent pathways.

Stronger Excitatory Drive Onto Interneurons Mediates Enhanced Inhibition in Thalamic Input

The finding that spike timing-dependent LTP in thalamo-amygdala pathway, as opposed to cortical input, could not be induced under conditions of intact $GABA_A$R-mediated inhibition, while both inputs were apparently identical in respect to the parameters of glutamatergic synaptic transmission, suggests that the convergent inputs might differ in their inhibition of principal neurons. To address this possibility, we recorded evoked EPSP/IPSP sequences in pyramidal cells (as evidenced by accommodating firing patterns; Figure 6A) under current-clamp conditions, with the stimulating electrodes placed to stimulate either cortical or thalamic input. As both principal neurons and local circuit interneurons in the LA receive glutamatergic inputs via fibers either in the external capsule (cortical pathway) or the internal capsule (thalamic pathway) (Figure 6D; Mahanty and Sah, 1998; Szinyei et al., 2000), stimulation of both inputs resulted in the appearance of biphasic synaptic responses in principal cells, consisting of the initial AMPAR-mediated EPSP that was followed by the PTX-sensitive $GABA_A$R-mediated inhibitory postsynaptic potential (IPSP, Figure 6B). The recorded neuron was depolarized by current injection through the recording electrode from a normal resting potential to -55 mV to increase the IPSP amplitude. The EPSP/IPSP sequence was blocked by the AMPAR antagonist CNQX (20 μM, Figure 6C). This confirms the disynaptic origin of the PTX-sensitive IPSP recorded in these inputs, providing feed-forward inhibition of principal neurons. The possible contribution of feed-back inhibition to the disynaptic IPSP was minimized by using a relatively low intensity of presynaptic stimulation that did not lead to the postsynaptic spike firing. The inputs did not differ in the voltage dependence of the IPSPs recorded over a wide range of membrane potentials, and reversal potential of the $GABA_A$R-mediated disynaptic IPSP was similar in both convergent inputs (Figures 6E and 6F).

To compare synaptic efficacy of inhibition in cortical input to that at thalamic pathway, the EPSP/IPSP sequences were elicited with increasing stimulation intensities in both inputs to the same neuron. The analysis of input-output curves for both monosynaptic glutamatergic EPSP and disynaptic GABAergic IPSP recorded in convergent inputs revealed that feed-forward inhibition is enhanced in thalamic pathway when compared to cortical input ($n = 9$;

ANOVA, $p < 0.001$; Figures 7A and 7B), while AMPA receptor EPSPs were not significantly different (ANOVA, $p = 0.32$).

What is the mechanism that could explain spatial asymmetry of inhibition in fear conditioning pathways? We found that paired pulse ratio (PPR) of the $GABA_AR$ IPSCs was not different in cortical and thalamic inputs to the LA. Disynaptic $GABA_AR$ IPSCs were recorded in voltage-clamp mode with the cesium-based intrapipette solution at a holding potential of 0mV. The initial component of the biphasic synaptic current, representing the monosynaptic AMPAR EPSC, did not make any detectable contribution to the evoked response under these conditions, as it was completely blocked by PTX (50 μM, Figures 7C and 7D). PPR at a 70-ms interval in cortical input was 1.05 ±0.04 (n = 17) compared with 0.98 ±0.04 (n = 15) in thalamic input (Figures 7E and 7F; no significant difference, t test, $p = 0.17$). Since PPR is a measure of presynaptic function, this finding indicates that the properties of GABA release were similar at both convergent pathways. Accordingly, the differential inhibitory control of synaptic transmission in two inputs could not be explained by the input-specific differences in probability of release of GABA-containing vesicles.

In agreement with a previous study (Szinyei et al., 2000), there was no significant difference between PPR values observed in the cortical input in response to stimulation with paired stimuli and PPR values obtained when stimulation of the thalamic input with a single stimulus was followed by a single pulse delivered to the cortical pathway (70-ms interstimulus interval; n = 6, t test, $p = 0.91$). This suggests that cortical and thalamic inputs converge on the same sub-population of interneurons in the LA.

Strengthening of excitatory glutamatergic inputs to interneurons leads to increased inhibition of principal cells in the LA (Mahanty and Sah, 1998). This suggests that input-specific differences in excitatory inputs to interneurons would result in different inhibitory drive in convergent pathways. To address this possibility, we obtained recordings of synaptic AMPAR EPSCs from interneurons in the presence of PTX (100 μM) evoked by stimulation of either cortical or thalamic input (Figure 8A). Recorded cells were identified as interneurons based on the non-accommodating firing behavior in response to prolonged depolarizing current injection (Figure 8B). Consistent with the earlier report (Szinyei et al., 2000), recorded interneurons always responded to stimulation of both pathways. We directly compared synaptic efficacy at convergent inputs to interneuron by analyzing input-output curves for the AMPAR EPSC. In these two-input experiments, the EPSCs were evoked in both pathways alternately by presynaptic stimuli of increasing intensity. We observed an increase in the slope of the input-output curves obtained in thalamic input, as compared to cortical pathway (Figure 8C; n = 5, ANOVA, $p < 0.001$). Synaptic enhancements in thalamic pathway were not associated with higher basal Pr, as we did not observe differences in paired-pulse ratio of the EPSC recorded at a 50-ms interstimulus interval between cortical and thalamic inputs to interneuron (Figures 8D and 8E, n = 4, t test, $p = 0.16$).

To explore the mechanisms underlying the enhanced synaptic efficacy in thalamic input to interneurons, we estimated the mean size of unitary EPSCs recorded in LA interneurons in response to stimulation of cortical and thalamic afferents. In these experiments, we employed an approach that relies on minimal stimulation of the presynaptic inputs (Tsvetkov et al., 2002,2004; see Experimental Procedures for technical details). The mean amplitude of unitary EPSCs (potency) was 19.6 ±2.6 pA (n = 6) and 30.5 ±4.2 pA (n = 6) in cortical and thalamic inputs to interneurons, respectively (significant difference between two inputs, t test, $p < 0.05$; Figures 8F and 8G). The inputs did not differ, however, in the average failure rate of unitary responses (average failure rate was 58.2 ±5.3 %, n =6 and 57.3 ±8.2 %, n =6, in cortical and thalamic inputs, respectively; t test, $p = 0.92$), confirming that probability of release was similar in both pathways. These findings are consistent with the notion that excitatory drive is stronger

in thalamic input to interneuron, as compared to convergent cortical input, and the enhanced synaptic efficacy at thalamic afferents is likely to mediate the observed differences in inhibitory inputs to LA neurons.

LTP at Thalamo-Amygdala Synapses Is Rescued by Weakening Excitatory Inputs to Interneurons

If enhanced synaptic efficacy at glutamatergic inputs to interneurons in thalamo-amygdala pathway mediates the observed input-specific differences in LTP, then LTP in thalamic input should be induced when inhibition is decreased to the level comparable to that at cortical input by depressing excitatory inputs to interneurons. We directly tested this prediction, taking advantage of the finding that AMPA receptors in glutamatergic inputs to interneurons in the LA do not contain GluR2 subunit and therefore can be selectively blocked by external polyamines (Mahanty and Sah, 1998). In agreement with this earlier study, addition of synthetic polyamine NHPP-spermine (5 μM) to the external solution resulted in approximately two-fold decrease in the amplitude of the disynaptic $GABA_A$R-mediated IPSPs recorded in principal neurons (Figure 9A; n = 4; the IPSP was reduced to 43 ±5% of its baseline value). Consistent with the role of feed-forward inhibition in LTP induction, we found that in the presence of NHPP-spermine (5 μM) in the bath solution (without PTX) LTP in thalamic input to the LA was rescued. Under these conditions, the EPSP was potentiated to 142.1 ±16% (n = 4) (Figures 9B and 9C; significantly different from the EPSP amplitude when LTP-inducing protocol was delivered without both PTX and NHPP-spermine in the bath solution, $p < 0.04$). In addition, we observed significant LTP at the thalamo-amygdala synapses without PTX in the bath solution, when the stronger inhibition in thalamic input was counteracted with postsynaptic depolarization to -20 mV during the induction. Thus 40 min after LTP-inducing stimulation the EPSP in thalamic input was potentiated to 135 ±10 % of the baseline value (n = 8; $p < 0.04$ vs. the EPSP amplitude when LTP-inducing protocol was delivered without PTX and postsynaptic depolarization; Supplemental Figure 1B).

Conversely, LTP in cortical input to the LA was blocked when we attempted to induce it in the presence of the $GABA_A$ receptor agonist muscimol (2 μM; Figures 9D). Under these conditions, the EPSP remained at 96.0 ±8% of the baseline amplitude 35 min after the LTP-inducing stimulation (n = 5, significantly different from control LTP at the cortico-amygdala synapses, $p < 0.02$; Figure 9E). These findings further strengthen the view that input-specific differences in the strength of inhibition could account for the observed spatial specificity of LTP at convergent cortical and thalamic pathways.

Some of our findings differ from the previously published results (Humeau et al., 2005). Therefore, we have also performed the experiments under conditions identical to those in the study by Humeau et al. (2005). Thus we tested the induction protocol used in this previous work, which consisted of 3 EPSPs paired with 3 APs (with the EPSP-to-AP delay of 4-8 ms) at 30 Hz, repeated 15 times at 0.2 Hz in the presence of PTX. We found that in cortical input this induction protocol, delivered at 30° C - 32° C, resulted in statistically significant potentiation of the EPSP to 126 ±8 % of its baseline amplitude (n = 9, $p < 0.05$; Supplemental Figure 1C). To further replicate the conditions in Humeau et al. (2005), we have also performed LTP experiments in cortical input with 2 mM Ca^{2+} and 1.3 mM Mg^{2+} in external solution using the same induction protocol at 30° C - 32° C. Surprisingly, the EPSP was still significantly potentiated to 131 ±10 % of the baseline amplitude (n = 9, $p < 0.05$; Supplemental Figure 1D).

As LTD in thalamic input was not observed with our induction protocol, we have also performed the experiments when the AP preceded the EPSP by 4-8 ms (“LTD protocol”) under conditions identical to those in the study of Humeau et al. (2005), including the induction protocol, perfusion temperature (30° C - 32° C) and Ca^{2+}/Mg^2 ratio. We found that 40 min after the delivery of the AP-EPSP paring protocol in the presence of PTX the thalamo-amygdala

EPSP remained at 108.8 ±14 % of the baseline amplitude (n = 8, not significantly different from the baseline EPSP amplitude, p = 0.26; Supplemental Figure 1E), indicating that LTD was not induced. We found, however, that in slices from 10-11 day-old rats, the delivery of the LTD protocol (same as above) led to significant LTD in thalamic input. The EPSP was depressed to 61.8 ±8.7 % of its baseline value (at 35-40 min after the induction, n = 4, significantly different from the baseline EPSP, $p < 0.01$; Supplemental Figure 2). This indicates that thalamo-amygdala synapses possess the ability to undergo spike-EPSP paring-induced LTD, but it diminishes with age.

Discussion

Our results provide evidence that spike timing-dependent LTP is induced in both cortical and thalamic pathways when $GABA_A$ receptor-mediated inhibition is blocked. With $GABA_A$R-mediated inhibition present, the EPSP-spike induction protocol does not lead to LTP in thalamic input, while LTP in cortical input, although diminished, still could be induced. The induction of LTP at glutamatergic synapses in different brain regions, including the amygdala, is regulated by the strength of $GABA_A$ receptor-mediated inhibition of principal neurons by interneurons (Steele and Mauk, 1999; Shumyatsky et al., 2002; Bissiere et al., 2003). Consistent with these previous observations, we found that a stronger inhibitory drive in thalamic pathway (as compared to the cortical input) was associated with decreased susceptibility of thalamo-amygdala synapses to spike timing-dependent LTP under conditions of intact inhibition.

These data indicate that spatial specificity of LTP mechanisms in fear conditioning pathways is, at least in part, determined by the differential inhibitory control at convergent synaptic inputs. Spatial specificity of spike timing-dependent LTP in the LA did not result from input-specific differences in basic mechanisms of glutamatergic synaptic transmission, as cortico-amygdala and thalamo-amygdala synapses were indistinguishable in their probability of release, quantal size, or relative contribution of NMDA receptors with different subunit composition to the integral NMDAR synaptic current. Similar to the conventional forms of LTP in the amygdala (Tsvetkov et al., 2002,2004), the induction of spike timing-dependent LTP in both auditory inputs to the LA is dependent on postsynaptic Ca^{2+} influx through NMDA glutamate receptors (also see Bauer et al., 2002). Therefore, the stronger inhibitory drive in thalamic pathway may hamper activation of NMDA receptors and affect the induction of LTP at thalamo-amygdala synapses, contributing to pathway specificity of long-term synaptic modifications in fear conditioning circuitry. The time window for induction of LTP in either pathway is narrow and LTP is only induced when the EPSP onset precedes the action potential in postsynaptic neuron by less than 10 ms. Interestingly, the time-locked feed-forward IPSP does not control the duration of the time window for the induction of LTP with the EPSP-AP paring protocol in cortical pathway, as it remains unchanged under conditions of blocked inhibition.

Our data imply that enhanced efficacy of feed-forward inhibition in the thalamic pathway, as compared to the cortico-amygdala input, results from a stronger excitatory drive to interneurons in thalamo-amygdala pathway. The enhanced synaptic strength in thalamic input to interneuron was, at least in part, mediated by a larger mean amplitude of unitary EPSCs (potency), as compared to convergent cortical input, while no difference was observed between inputs in the probability of neurotransmitter release. It is possible that synaptic enhancements in thalamic input are also underlain by either a denser innervation of each given interneuron (also receiving cortical afferents) in this pathway, or a larger number of synapses formed on each interneuron by individual axons, while the overall number of afferent fibers activated in each pathway is similar. Alternatively, the observed differences in inhibition could arise from input-specific activation of the spatially segregated clusters of interneurons. If one of the inputs recruits a larger number of interneurons, this could provide a mechanism of differential inhibitory control

of principal neurons. However, we observed cross-interaction between $GABA_AR$-mediated responses in convergent thalamic and cortical inputs confirming a previously reported finding that both pathways always converge on same interneurons in the LA (Szinyei et al., 2000). Enhanced excitatory drive into interneurons in thalamic pathway, as compared to cortical input converging on same interneurons, would result in an increased probability of spike firing in interneurons in response to activation of thalamic afferents. Consistent with this, we found that the feed-forward GABAergic IPSP is significantly larger in thalamic input, thus preventing the induction of LTP in this pathway when inhibition is not blocked.

The direction and magnitude of synaptic modifications during spike timing-dependent plasticity critically depends on a relative order of pre- and postsynaptic activation and time interval between pre- and postsynaptic action potential firing (Markram et al., 1997; Sjostrom et al., 2001; Bi and Poo, 2001; Bi and Rubin, 2005). We found that when the AP precedes the EPSP, the repetitive AP-EPSP pairing does not lead to LTD at naïve synapses, in either cortical or thalamic pathway. The lack of LTD was observed with a wide range of delays between the postsynaptic (AP) and presynaptic (EPSP) stimuli both with and without $GABA_AR$-mediated inhibition present. Thus synapses in afferent inputs to the LA utilize a form of the temporally asymmetric learning rule under which the strength of activated synapses would only be modified when the postsynaptic action potential closely follows the synaptic input. The lack of LTD with the “post-before-pre” induction protocol in slices from 3-5 week-old rats, regardless of the delay duration between the AP and EPSP or frequency of presynaptic stimulation, could reflect a developmental profile of LTD which is shown to be most prominent at early postnantal stages and steeply diminishes with age (Bolshakov and Siegelbaum, 1994). Consistent with this, we observed significant LTD of the thalamo-amygdala EPSP induced with the AP-EPSP paring protocol in slices from 10-11 day-old rats.

Our findings are in contradiction to the results of a recently published study providing evidence that under conditions of blocked inhibition STDP in mouse brain slices could only be observed in thalamic input to the LA, while cortico-amygdala synapses were not modified by brief periods of coincident pre- and postsynaptic spiking (Humeau et al., 2005). Moreover, this previous study suggested that pathway specificity of STDP in the amygdala could be explained by morphological and functional differences between dendritic spines contacted by convergent cortical and thalamic afferents. Although our results do not exclude a possibility that under certain conditions spine-specific mechanisms could contribute to the spatial heterogeneity of LTP, they indicate that spike timing-dependent LTP of identical magnitude could be induced in either pathway when inhibition is blocked (also see Shumyatsky et al., 2005). Moreover, in the present study, we observed significant LTP at the cortico-amygdala synapses under the same experimental conditions (LTP induction protocol, perfusion temperature, external Ca^{2+} to Mg^{2+} ratio) as in Humeau et al. (2005) (see Supplemental Figure 1). The reasons for the inconsistency of results are unclear, although it is still possible that some subtle differences in experimental conditions, which are difficult to account for (e.g., quality of slices or precise placement of stimulation and recording pipettes), could contribute to the discrepancies between two studies.

It has become increasingly evident that different synapses in a neural circuit of a learned behavior may utilize learning rules that are optimized for specific functions. For example, recordings from single fusiform or cartwheel cells of the dorsal cochlear nucleus in slices of mouse brainstem revealed that synaptic learning rules could vary depending on the type of postsynaptic target (Tzounopoulos et al., 2004). Glutamatergic inputs to fusiform cells exhibited canonical spike timing-dependent plasticity: the EPSP-AP paring protocol resulted in LTP, while the AP-EPSP (reversed order) protocol produced LTD of synaptic transmission. In contrast, the EPSP-AP protocol resulted in LTD at inputs to cartwheel cells, while the AP-EPSP protocol did not produce any changes in synaptic strength. A similar learning rule was

described at synapses between parallel fibers and Purkinje-like cells of the electrosensory lobe of mormyrid electric fish (Han et al., 2000). In this study the EPSP-AP protocol also led to LTD of synaptic transmission, while the induction of spikes before the EPSPs failed to induce plasticity. This is consistent with the notion that numerous forms of synaptic plasticity may exist at central synapses to achieve optimal network dynamics required for efficient memory retention.

Together, the reported findings demonstrate spatiotemporal specificity of synaptic plasticity at convergent cortico-amygdala and thalamo-amygdala pathways, conveying to the LA information about the CS from the auditory cortex and auditory thalamus, respectively, during fear learning. This complements a recent study of LTP in auditory inputs to the LA in freely moving rats which suggested differential roles for thalamic and cortical auditory inputs in long-term fear memory (Doyere et al., 2003). Our data do not imply, however, that learning-associated synaptic modifications in thalamic input to the LA play a less significant role in fear conditioning than LTP in the cortico-amygdala pathway. According to a previously proposed probabilistic model, computation in neural networks might implicate operations leading to decorrelation of convergent sensory inputs or reduction of redundancy of incoming information (reviewed by Destexhe and Marder, 2004). Thus spatial asymmetry of synaptic plasticity could provide an efficient mechanism for reduction of information flow redundancy in two convergent inputs resulting in the specific output pattern of neurons in the LA. Input specific differences in LTP mechanisms could also contribute to directionality of the information flow in fear conditioning pathways providing a means for the CS discrimination during fear memory retrieval.

Experimental Procedures

Amygdala slices (250-300 μm) were prepared from 3-5 week old Sprague-Dawley rats with a vibratome. Slices were continuously superfused in solution containing (in mM): 119 NaCl, 2.5 KCl, 2.5 $CaCl_2$, 1.0 $MgSO_4$, 1.25 NaH_2PO_4, 26.0 $NaHCO_3$, 10 glucose, and 0.1 picrotoxin (unless noted otherwise) and equilibrated with 95% O_2 and 5% CO_2 (pH 7.3-7.4) at room temperature (22° C - 24°). Whole-cell recordings of compound EPSCs/EPSPs or IPSCs/IPSPs were obtained from either pyramidal cells or interneurons in the dorsolateral division of the lateral amygdala under visual guidance (DIC/infrared optics) with an EPC-9 amplifier and Pulse v8.40 software (HEKA Elektronik). Synaptic responses were evoked by stimulation of the fibers either in the external capsule (cortical input) or in the internal capsule (thalamic input) at 0.05 Hz. The evoked GABA-mediated monosynaptic IPSCs were elicited in the presence of CNQX (20 μM) by the stimulation electrode placed within the lateral nucleus of the amygdala to directly stimulate interneurons. The asynchronous EPSCs were recorded under conditions when evoked release was desynchronized by substitution of Sr^{2+} for extracellular Ca^{2+} (Oliet et al. 1996) and analysed with the Mini Analysis Program (Synaptosoft Inc., Decatur, GA). The patch electrodes (3-5 MΩ resistance) in all current-clamp experiments contained (in mM): 120 K-gluconate, 5 NaCl, 1 $MgCl_2$, 0.2 EGTA, 10 HEPES, 2 MgATP, and 0.1 NaGTP (adjusted to pH 7.2 with KOH). In all voltage-clamp experiments, 120 mM Cs-methane-sulfonate was used instead of K-gluconate. Currents were filtered at 1 kHz and digitized at 5 kHz. Unitary EPSCs were evoked by low-intensity current pulses (20-60 μA; 100 μs duration) applied through a fine-tipped (~2 μM), concentric stimulating electrode consisting of a patch pipette that was coated with silver paint (Tsvetkov et al., 2002). The stimulating pipettes were positioned to activate either cortical or thalamic input to the LA (Supplemental Figure 1A). The recording was used if the mean EPSC amplitude showed a steep all-or-none threshold as a function of stimulating current intensity, and if there was no change in potency (the mean size of responses, excluding failures of synaptic transmission) during double-pulse stimulation with a 50 ms interpulse interval. In all LTP experiments, the stimulus intensity was adjusted to produce synaptic responses with an amplitude which was ~20-25% of maximum amplitude

EPSP. Since we controlled for the size of the baseline EPSP, the induction conditions were identical for all LTP groups. For induction of LTP, 80 presynaptic stimuli, delivered at 2 Hz either to the external capsule fibers (cortical input) or to the internal capsule fibers (thalamic input), were paired with action potentials evoked in a postsynaptic cell with a controlled delay from the onset of each EPSP, as previously described (Shumyatsky et al., 2005). Action potentials were induced by short depolarizing current injections. Summary LTP graphs were constructed by normalizing data in 60 s epochs to the mean value of the baseline EPSP.

Supplementary Material

Refer to Web version on PubMed Central for supplementary material.

ACKNOWLEDGEMENTS

We thank Yan Li and Keith Tully for constructive discussions. Evgeny Tsvetkov was on leave from Sechenov Institute of Evolutionary Physiology and Biochemistry, Russian Academy of Sciences. This study was supported by NIH grants NS44185, NS045625 and DA15098 (V.Y.B.), the Esther A. and Joseph Klingenstein Fund (V.Y.B.) and by the National Alliance for Research on Schizophrenia and Depression (V.Y.B.).

References

Bauer EP, LeDoux JP, Nader K. Fear conditioning and LTP in the lateral amygdala are sensitive to the same stimulus contingencies. Nat. Neurosci 2001;4:687–688. [PubMed: 11426221]

Bauer EP, Schafe GE, LeDoux JE. NMDA receptors and L-type voltage-gated calcium channels contribute to long-term potentiation and different components of fear memory formation in the lateral amygdala. J. Neurosci 2002;22:5239–5249. [PubMed: 12077219]

Bi G, Poo M. Synaptic modification by correlated activity: Hebb's postulate revisited. Annu. Rev. Neurosci 2001;24:139–166. [PubMed: 11283308]

Bi G, Rubin J. Timing in synaptic plasticity: from detection to integration. Trends in Neurosci 2005;28:222–228.

Bissiere S, Humeau Y, Luthi A. Dopamine gates LTP induction in lateral amygdala by suppressing feedforward inhibition. Nat. Neurosci 2003;6:587–592. [PubMed: 12740581]

Bolshakov VY, Siegelbaum SA. Postsynaptic induction and presynaptic expression of hippocampal long-term depression. Science 1994;264:1148–1152. [PubMed: 7909958]

Campeau S, Davis M. Involvement of subcortical and cortical afferents to the lateral nucleus of the amygdala in fear conditioning measured with fear-potentiated startle in rats trained concurrently with auditory and visual conditioned stimuli. J. Neurosci 1995;15:2312–2327. [PubMed: 7891169]

Davis M, Whalen PJ. The amygdala: vigilance and emotion. Mol. Psychiatry 2001;6:13–34. [PubMed: 11244481]

Destexhe A, Marder A. Plasticity in single neuron and circuit computation. Nature 2004;431:789–795. [PubMed: 15483600]

Doyere V, Schafe GE, Sigurdsson T, LeDoux JE. Long-term potentiation in freely moving rats reveals asymmetries in thalamic and cortical inputs to the lateral amygdala. Eur. J. Neurosci 2003;17:2703–2715. [PubMed: 12823477]

Fanselow MS, Poulos AM. The neuroscience of mammalian associative learning. Annu. Rev. Psychol 2005;56:207–234. [PubMed: 15709934]

Feldman DE. Timing-based LTP and LTD at vertical inputs to layer II/III pyramidal cells in rat barrel cortex. Neuron 2000;27:45–56. [PubMed: 10939330]

Goosens KA, Hobin JA, Maren S. Auditory-evoked spike firing in the lateral amygdala and Pavlovian fear conditioning: mnemonic code or fear bias? Neuron 2003;40:1013–1022. [PubMed: 14659099]

Han VZ, Grant K, Bell CC. Reversible associative depression and nonassociative potentiation at a parallel fiber synapse. Neuron 2000;27:611–622. [PubMed: 11055442]

Hessler NA, Shirke AM, Malinow R. The probability of transmitter release at a mammalian central synapse. Nature 1993;366:569–572. [PubMed: 7902955]

Huang YY, Kandel ER. Postsynaptic induction and PKA-dependent expression of LTP in the lateral amygdala. Neuron 1998;21:169–178. [PubMed: 9697861]

Huettner JE, Bean BP. Block of N-methyl-D-aspartate-activated current by the anticonvulsant MK-801: selective binding to open channels. Proc. Natl. Acad. Sci. USA 1988;85:1307–1311. [PubMed: 2448800]

Humeau Y, Herry C, Kemp N, Shaban H, Fourcaudot E, Bissiere S, Luthi A. Dendritic spine heterogeneity determines afferent-specific Hebbian plasticity in the amygdala. Neuron 2005;45:119–131. [PubMed: 15629707]

Karmarkar UR, Najarian MT, Buonomano DV. Mechanisms and significance of spike-timing dependent plasticity. Biol. Cybern 2002;87:373–382. [PubMed: 12461627]

LeDoux JE. Emotion circuits in the brain. Annu. Rev. Neurosci 2000;23:155–184. [PubMed: 10845062]

Liu L, Wong TP, Pozza MF, Lingenhoehl K, Wang Y, Sheng M, Auberson YP, Wang YT. Role of NMDA receptor subtypes in governing the direction of hippocampal synaptic plasticity. Science 2004;304:1021–1024. [PubMed: 15143284]

Lopez de Armenia M, Sah P. Development and subunit composition of synaptic NMDA receptors in the amygdala: NR2B synapses in the adult central amygdala. J. Neurosci 2003;23:6876–6883. [PubMed: 12890782]

Mahanty NK, Sah P. Calcium-permeable AMPA receptors mediate long-term potentiation in interneurons in the amygdala. Nature 1998;394:683–687. [PubMed: 9716132]

Maren S. Neurobiology of Pavlovian fear conditioning. Annu. Rev. Neurosci 2001;24:897–931. [PubMed: 11520922]

Maren S, Quirk GJ. Neuronal signaling of fear memory. Nat. Rev. Neurosci 2004;5:844–852. [PubMed: 15496862]

Markram H, Lubke J, Frotscher M, Sakmann B. Regulation of synaptic efficacy by coincidence of postsynaptic APs and EPSPs. Science 1997;275:213–215. [PubMed: 8985014]

McKernan MG, Shinnick-Gallagher P. Fear conditioning induces a lasting potentiation of synaptic currents in vitro. Nature 1997;390:607–611. [PubMed: 9403689]

Neyton J, Paoletti P. Relating NMDA Receptor Function to Receptor Subunit Composition: Limitations of the Pharmacological Approach. J. Neurosci 2006;26:1331–1333. [PubMed: 16452656]

Oliet SH, Malenka RC, Nicoll RA. Bidirectional control of quantal size by synaptic activity in the hippocampus. Science 1996;271:1294–1297. [PubMed: 8638114]

Pitkanen A, Savander V, LeDoux JE. Organization of intra-amygdaloid circuitries in the rat: an emerging framework for understanding functions of the amygdala. Trends Neurosci 1997;20:517–523. [PubMed: 9364666]

Rogan MT, Staubli UV, LeDoux JE. Fear conditioning induces associative long-term potentiation in the amygdala. Nature 1997;390:604–607. [PubMed: 9403688]

Szinyei C, Heinbockel T, Montagne J, Pape HC. Putative cortical and thalamic inputs elicit convergent excitation in a population of GABAergic interneurons of the lateral amygdala. J. Neurosci 2000;20:8909–8915. [PubMed: 11102501]

Shumyatsky GP, Tsvetkov E, Malleret G, Vronskaya S, Hatton M, Hampton L, Battey JF, Dulac C, Kandel ER, Bolshakov VY. Identification of a signaling network in lateral nucleus of amygdala important for inhibiting memory specifically related to learned fear. Cell 2002;111:905–918. [PubMed: 12526815]

Shumyatsky GP, Malleret G, Shin RM, Tully K, Takizawa S, Tsvetkov E, Joseph J, Vronskaya S, Yin DQ, Schubart UK, Kandel ER, Bolshakov VY. Stathmin, a gene enriched in the amygdala, controls both learned and innate fear. Cell 2005;123:697–709. [PubMed: 16286011]

Sjostrom PJ, Turrigiano GG, Nelson SB. Rate, timing, and cooperativity jointly determine cortical synaptic plasticity. Neuron 2001;32:1149–1164. [PubMed: 11754844]

Steele PM, Mauk MD. Inhibitory control of LTP and LTD: stability of synapse strength. J Neurophysiol 1999;81:1559–1566. [PubMed: 10200191]

Tsvetkov E, Carlezon WA, Benes FM, Kandel ER, Bolshakov VY. Fear conditioning occludes LTP-induced presynaptic enhancement of synaptic transmission in the cortical pathway to the lateral amygdala. Neuron 2002;34:289–300. [PubMed: 11970870]

Tsvetkov E, Shin RM, Bolshakov VY. Glutamate uptake determines pathway specificity of long-term potentiation in the neural circuitry of fear conditioning. Neuron 2004;41:139–151. [PubMed: 14715141]

Tzounopoulos T, Kim Y, Oertel D, Trussell LO. Cell-specific, spike timing-dependent plasticities in the dorsal cochlear nucleus. Nat. Neurosci 2004;7:719–725. [PubMed: 15208632]

Wang HX, Gerkin RC, Nauen DW, Bi GQ. Coactivation and timing-dependent integration of synaptic potentiation and depression. Nat. Neuosci 2005;8:187–193.

Weisskopf MG, Bauer EP, LeDoux JE. L-type voltage-gated calcium channels mediate NMDA-independent associative long-term potentiation at thalamic input synapses to the amygdala. J. Neurosci 1999;19:10512–10519. [PubMed: 10575047]

Xu-Friedman MA, Regehr WG. Probing fundamental aspects of synaptic transmission with strontium. J. Neurosci 2000;20:4414–4422. [PubMed: 10844010]

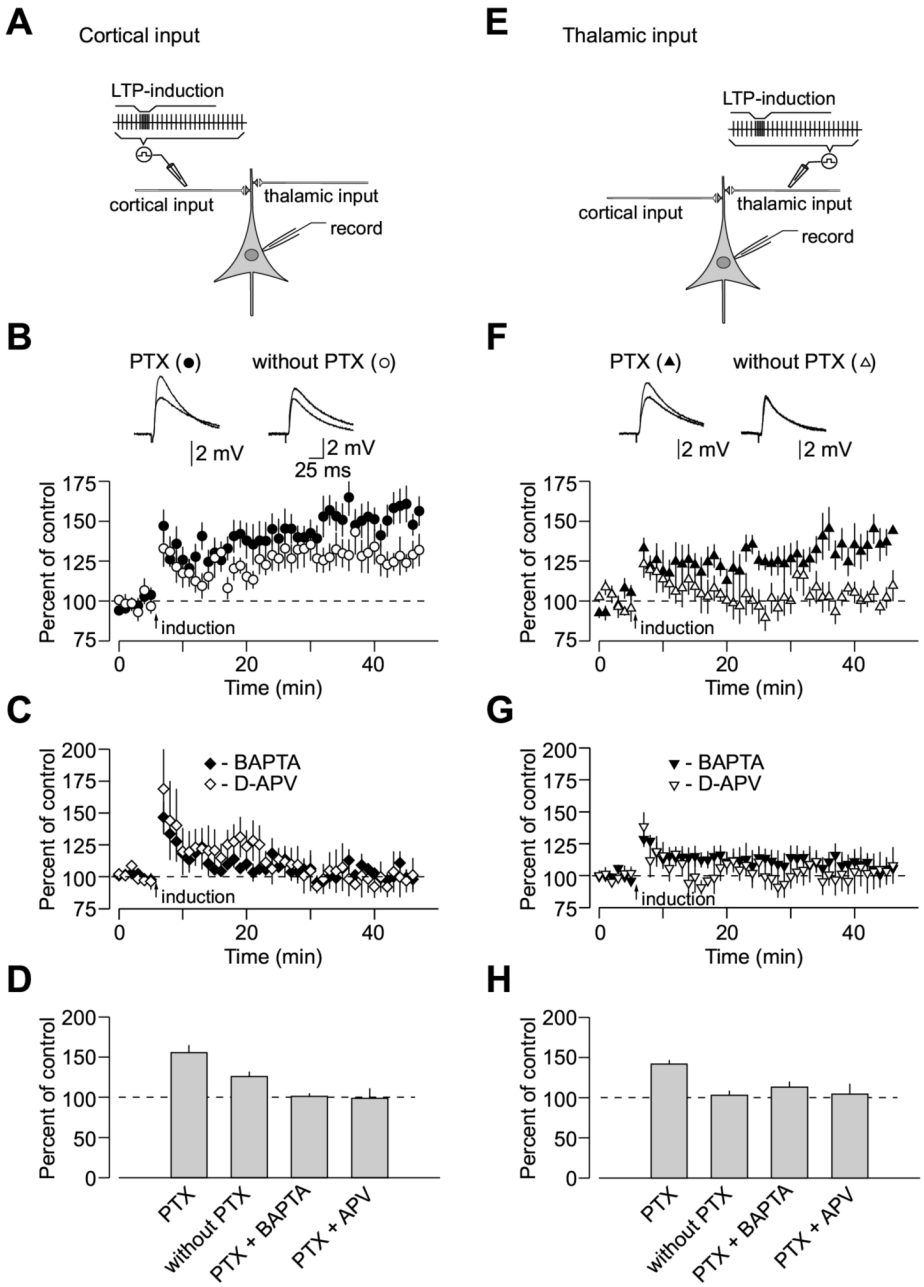

Figure 1.

Properties of Spike Timing-Dependent LTP at the Cortico-Amygdala and Thalamo-Amygdala Synapses. (**A**) A schematic representation of the experimental design when cortical input was individually activated, showing the position of the recording and stimulation electrodes. (**B**) Summary graphs of the LTP experiments in cortical input in the presence of PTX (100 μM, mean ±SEM; n = 12) and without PTX (n = 9) in the bath solution. To induce LTP, 80 EPSPs were evoked at a frequency of 2 Hz; each EPSP was paired with action potential induced in a recorded neuron with 4-8 ms delay from the onset of the EPSP by short depolarizing current injections through the recording electrode. Insets show the average of 10 EPSPs recorded in individual experiments before and 35 min after the LTP-inducing stimulation (arrow) with

PTX (left) or without PTX (right) in the bath solution. (**C**) LTP in cortical input is blocked by D-APV (50 μM, n = 4) in the external solution or when a high concentration of Ca^{2+} chelator BAPTA (10mM) is included in the recording pipette solution (n = 4). (**D**) Summary of LTP experiments (mean ±SEM) at cortico-amygdala synapses. (**E**) A schematic representation of the experimental design in thalamic pathway. (**F**) Summary graphs of the LTP experiments in thalamic input in the presence of PTX (n = 6) and without PTX (n = 5) in the bath solution. Insets show the average of 10 thalamo-amygdala EPSPs recorded in individual experiments before and 35 min after the LTP-inducing stimulation with PTX (left) or without PTX (right) in the bath solution. (**G**) LTP in thalamic input is blocked by D-APV (50 μM, n = 6) in the bath solution or by BAPTA (10mM) in the recording pipette solution (n = 10). (**H**) Summary of LTP experiments (mean ±SEM) at thalamo-amygdala synapses.

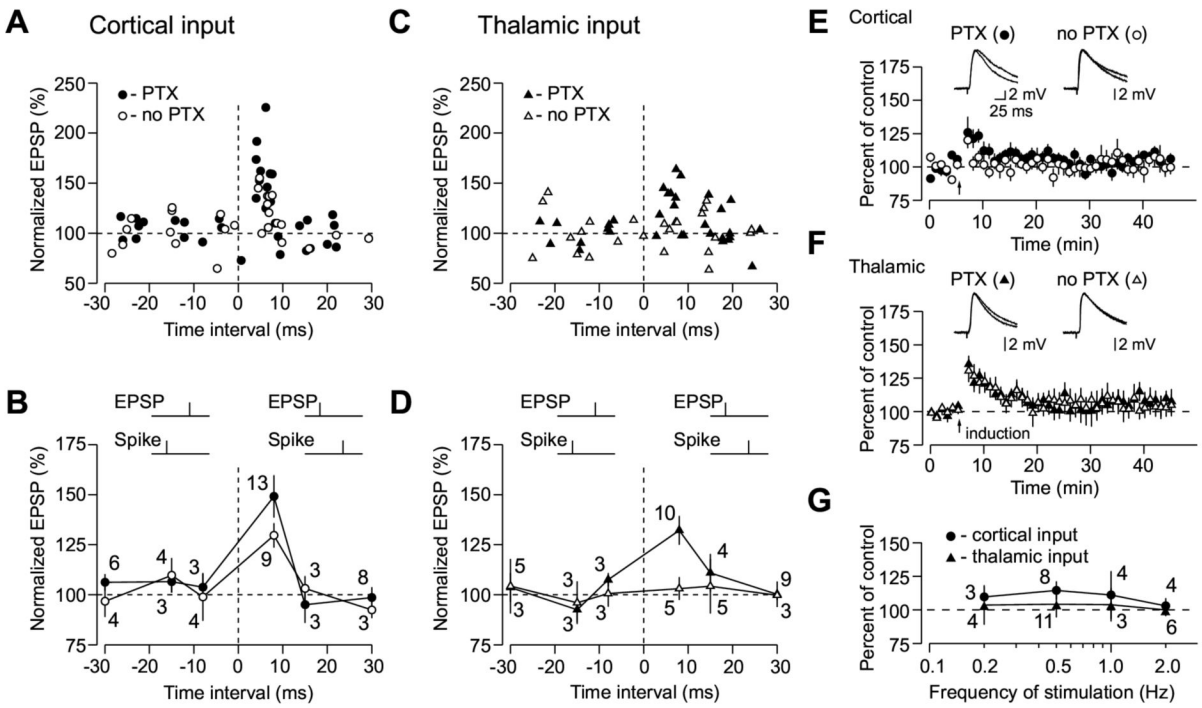

Figure 2.

Time Window for the Induction of Spike Timing-Dependent Plasticity in the LA Is Asymmetric. (**A**) Summary of the percentage change in the amplitude of the cortico-amygdala EPSP 35-40 min after correlated pre- and postsynaptic activation when either the EPSP preceded action potential in a postsynaptic neuron (x-axis, positive time intervals) or AP preceded the EPSP (x-axis, negative time intervals), with or without PTX in the bath solution. Time intervals were determined between the onset of the EPSP and the peak of the postsynaptic AP. Each data point represents an individual experiment. (**B**) Summary of LTP experiments in cortical input as in (A) using positive time intervals of 0 to +8 ms, greater than +8 to +15 and greater than +15 to +30 ms or negative time intervals of 0 to -8 ms, greater than -8 ms to -15 ms and greater than -15 ms to -30 ms. The number of experiments is indicated for each time window. (**C**) Summary of the percentage change in the amplitude of the thalamo-amygdala EPSP 35-40 min after correlated pre- and postsynaptic activation (same experimental procedure as in A), with or without PTX in the bath solution. (**D**) Summary of LTP experiments in thalamic input as in (C) using positive time intervals of 0 to +8 ms, greater than +8 to +15 and greater than +15 to +30 ms or negative time intervals of 0 to -8 ms, greater than -8 ms to -15 ms and greater than -15 ms to -30 ms. (**E**) Summary graphs of all experiments in cortical input when AP preceded the EPSP (negative time intervals) in the presence of PTX (100 μM, mean ±SEM; n = 12) and without PTX (n = 12) in the bath solution. Traces are averages of 10 EPSPs recorded in individual experiments before and 30 min after the repetitive AP-EPSP pairing (arrow) with PTX (left) or without PTX (right) in the bath solution. (**F**) Summary graphs of all experiments in thalamic input when AP preceded the EPSP in the presence of PTX (n = 9) and without PTX (n = 11) in the bath solution. (**G**) Effects of the repetitive AP-EPSP paring with interpulse delays of -5 to -15 ms on the amplitude of the EPSP, expressed as the percentage change relative to the baseline value, when same number of the AP-EPSP pairs (80) was

induced at four different frequencies (0.2 Hz, 0.5 Hz, 1 Hz, 2 Hz; x-axis, logarithmic scale) in cortical and thalamic inputs with PTX in the external solution.

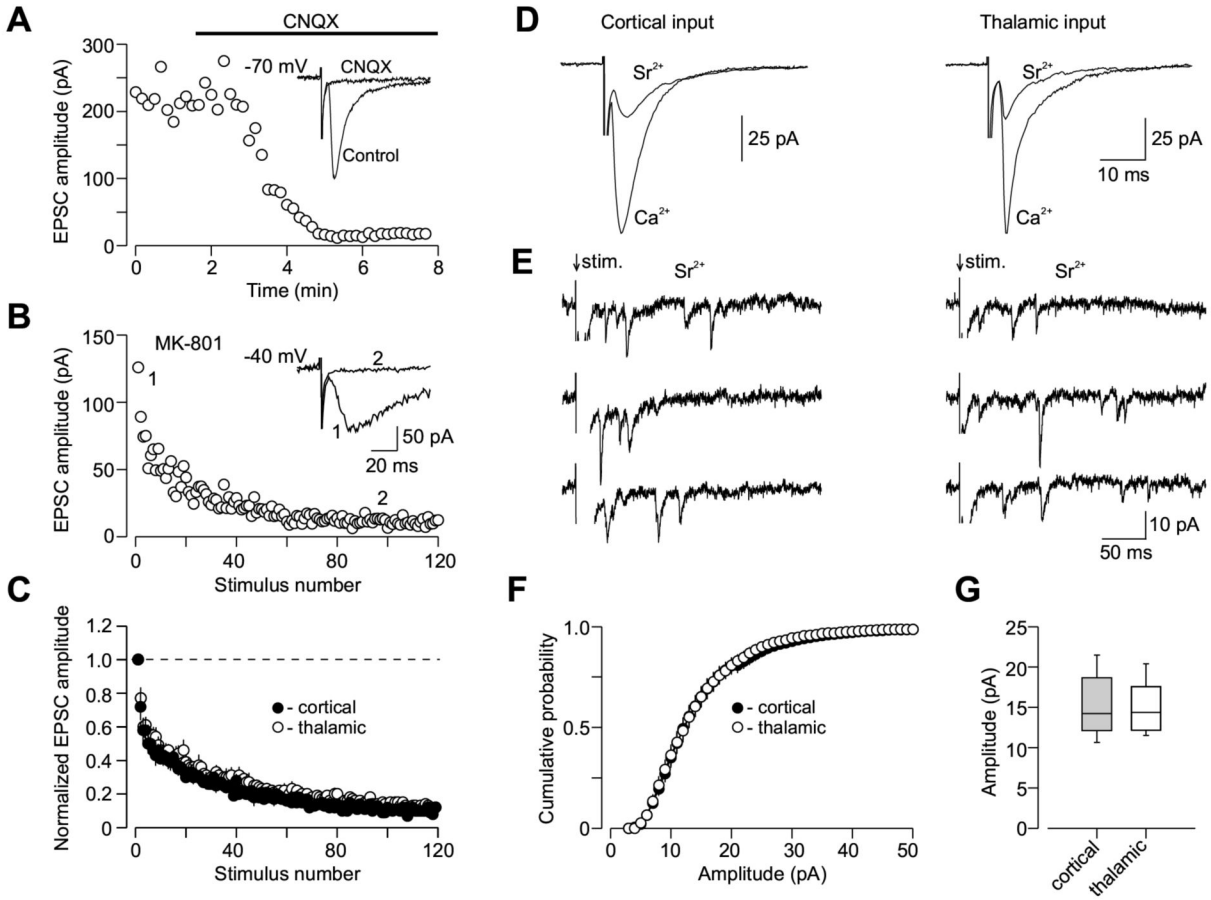

Figure 3.

Quantal Parameters of Glutamatergic Synaptic Transmission at Cortical and Thalamic Pathways. (**A**) Evoked cortico-amygdala EPSCs were blocked by bath application of 20 μM CNQX at a holding potential of -70 mV. (**B**) The progressive block by MK-801 (40 μM) of the NMDA receptor EPSC recorded in the presence of CNQX at a holding potential of -40 mV. MK-801 was applied to the slice in the absence of presynaptic stimulation for 10 min. To measure rate of MK-801 block, the external capsule was stimulated at 0.1 Hz frequency. Inset shows the baseline NMDAR EPSC (1) and its block at the end of presynaptic stimulation in the presence of MK-801 (2). (**C**) Summary graphs of the experiments with MK-801 protocol in cortical (n = 9) and thalamic (n = 9) inputs. In each individual experiment, EPSC amplitudes were normalized by the first EPSC. Data points show mean ±SEM. (**D**) The amplitude of the AMPAR EPSC recorded either in cortical (left) or thalamic (right) inputs at a holding potential of -70 mV was significantly reduced, when Sr^{2+} was substituted for extracellular Ca^{2+}. (**E**) Representative traces of the asynchronous quantal EPSCs evoked by stimulation (at arrow) of cortical (left) or thalamic (right) inputs. (**F**) Cumulative amplitude histograms of asynchronous quantal events recorded either at cortical (n = 10) or thalamic (n = 12) pathways. (**G**) Summary box plots of asynchronous EPSC data in cortical and thalamic inputs. The line inside the boxes marks the median, and the box boundaries indicate the 25^{th} and 75^{th} percentiles. The error bars indicate the 10^{th} and 90^{th} percentiles.

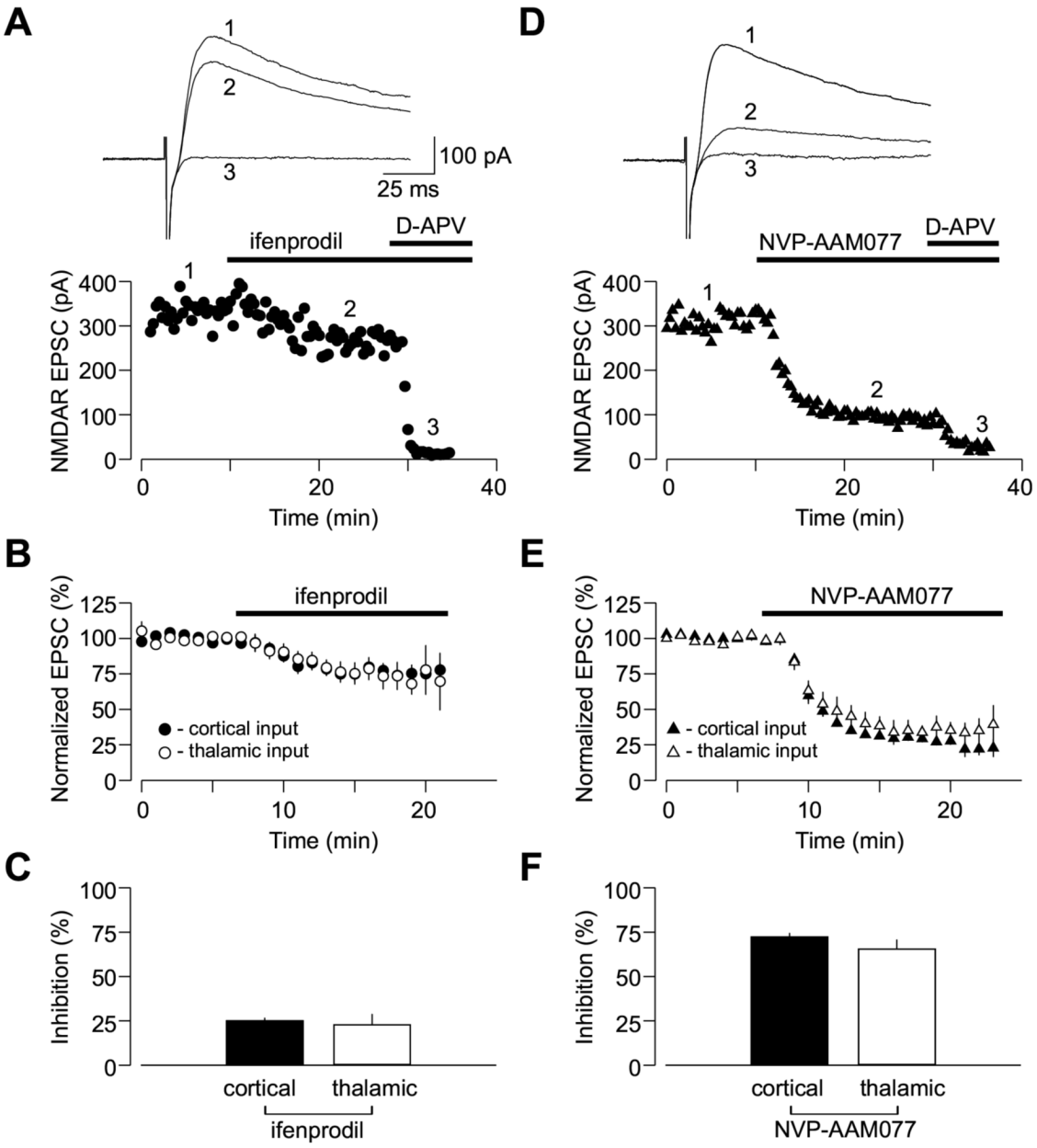

Figure 4.

Convergent Cortical and Thalamic Inputs Do Not Differ in Subunit Composition of Synaptic NMDA Receptors. (**A**) Application of ifenprodil (10 μM) moderately depressed the isolated NMDAR EPSC recorded in the presence of CNQX at a holding potential of +50 mV in cortical input. Subsequent addition of D-APV (50 μM) completely blocked the EPSC. Insets show the averages of 10 NMDAR EPSCs recorded under baseline conditions (1), during ifenprodil-induced depression (2) and after D-APV application (3). (**B**) Averaged graphs of the experiments involving ifenprodil application as in (A) in cortical input (n = 5) and thalamic input (n = 5). Graphs were obtained by normalizing data in 60 s epochs to the mean value of the baseline (pre-drug) NMDAR EPSC (mean ±SEM). (**C**) Summary of the ifenprodil effects

on the NMDAR EPSC at cortical and thalamic pathways. (**D**) Application of NVP-AAM077 (0.5 μM) significantly depressed the isolated NMDAR EPSC recorded at a holding potential of +50 mV in cortical input. Insets show the averages of 10 NMDAR EPSCs recorded under baseline conditions (1), during NVP-AAM077-induced depression (2) and after D-APV application (3). NVP-AAAM077 was a generous gift from Novartis Pharma AG (Switzerland). (**E**) Averaged graphs of the experiments involving NVP-AAM077 application as in (D) in cortical input (n = 8) and thalamic input (n = 7). (**F**) Summary of the NVP-AAM077 effects on the NMDAR EPSC at cortical and thalamic pathways (mean ±SEM).

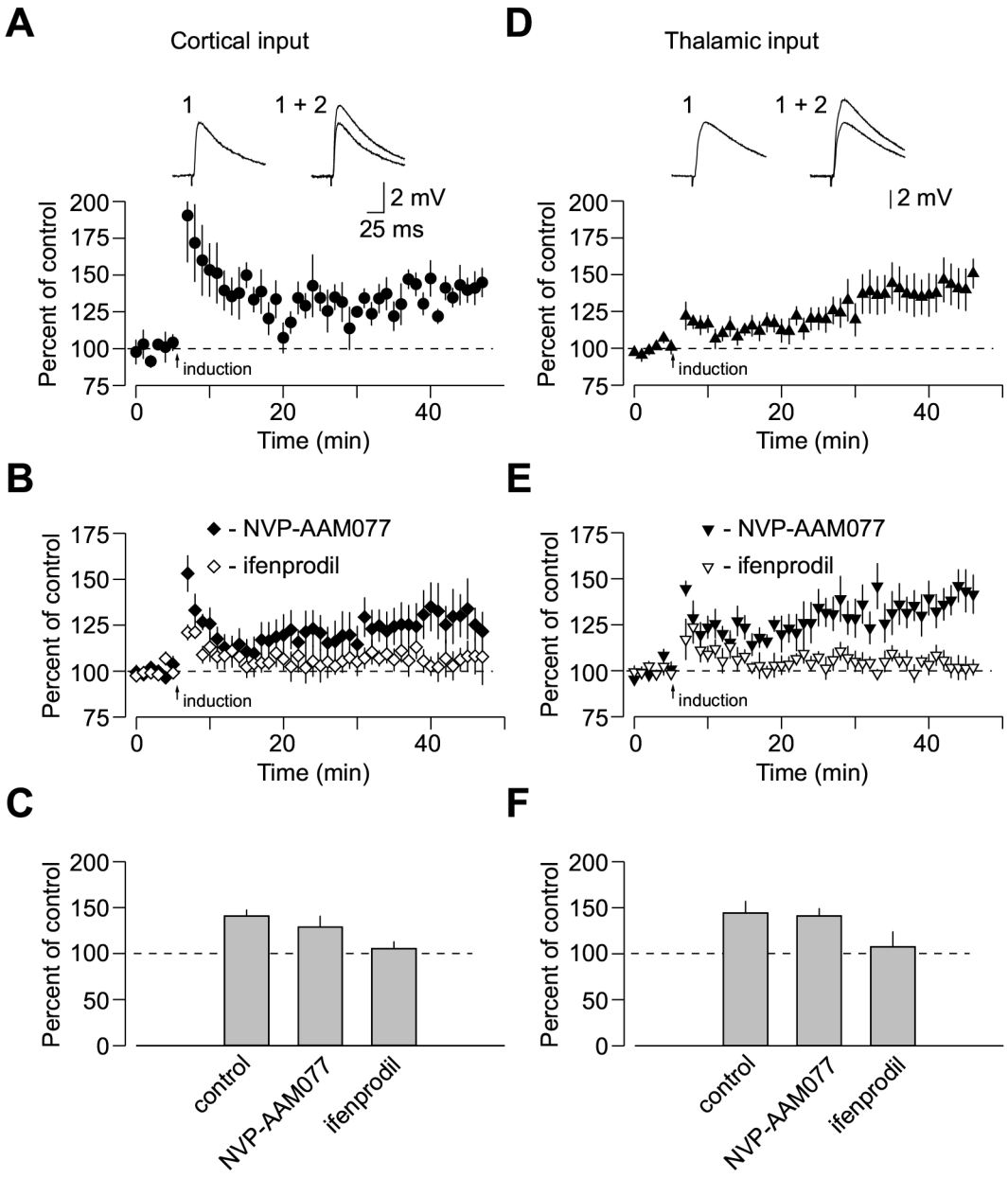

Figure 5.

Evidence that Activation of Synaptic NR2B-Containing NMDA Receptors Accounts for the Induction of Spike Timing-Dependent LTP in Cortical and Thalamic Inputs. (**A**) LTP at cortico-amygdala pathway induced by the repetitive EPSP-AP paring using positive time intervals of +4 to +6 ms between the onset of the EPSP and the AP peak (n = 5) with PTX in the bath solution. Insets show the average of 10 EPSPs recorded before (1) and 35 min after (2) the EPSP-AP pairing procedure. (**B**) Effects of ifenprodil (10 μM, n = 9) and NVP-AAM077 (0.5 μM, n = 6) on spike timing-dependent LTP in cortical input. (**C**) Summary of LTP experiments in cortical input shown in (A) and (B) (mean ±SEM). (**D**) LTP at thalamo-amygdala pathway (n = 8) induced with PTX in the bath solution. Insets show the average of

10 EPSPs recorded before (1) and 35 min after (2) the EPSP-AP pairing procedure. (**E**) Effects of ifenprodil (n = 5) and NVP-AAM077 (n = 6) on spike timing-dependent LTP in thalamic input. (**F**) Summary of LTP experiments in thalamic input shown in (D) and (E) (mean ±SEM).

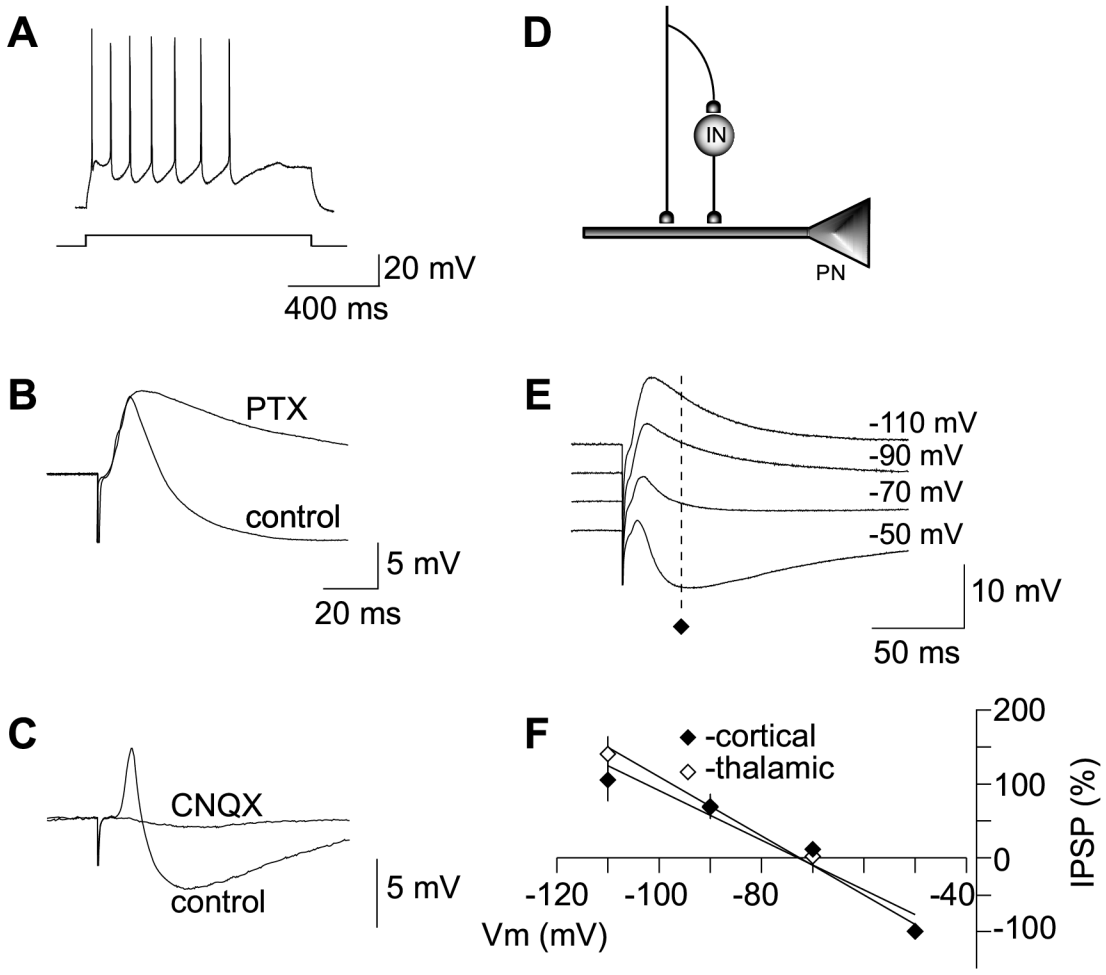

Figure 6.

The EPSP/IPSP Sequences in the Cortical and Thalamic Inputs to the LA neuron. (**A**) Response of a cell in the LA to prolonged depolarizing current injection. Significant spike frequency accommodation observed in the recorded cell indicates that it is a pyramidal neuron. (**B**) Biphasic synaptic response recorded under current-clamp conditions in the LA neuron at -55 mV (control) in response to stimulation of cortical input. It consisted of the initial EPSP that was followed by the PTX-sensitive IPSP. A second trace (PTX) depicts an isolated EPSP when the IPSP was blocked with PTX. (**C**) The ESPS/IPSP sequence (control) was blocked by CNQX (20 μM), indicating the IPSP is disynaptic. (**D**) A schematic representation of the neural circuit for the EPSP/IPSP sequences in the LA. IN, interneuron; PN, principal neuron. (**E**) The EPSP/IPSP sequences recorded in cortical input over a range of membrane potentials (from -110 mV to -50 mV). Each trace represents the average of 10 responses. Dashed line marks the peak amplitude of the IPSP. (**F**) Dependence of the IPSP amplitude on membrane potential when responses were evoked either at cortical (n = 6) or thalamic pathway (n = 6). Values for the graph were obtained by normalizing the peak IPSP amplitude at each membrane potential to the amplitude of the IPSP recorded at -50 mV. Reversal potential of the IPSP was -71.3 ±4.0 mV (n = 6) and -72.1 ±3.7 mV (n = 6) in cortical and thalamic inputs, respectively (no significant difference between inputs, p = 0.89).

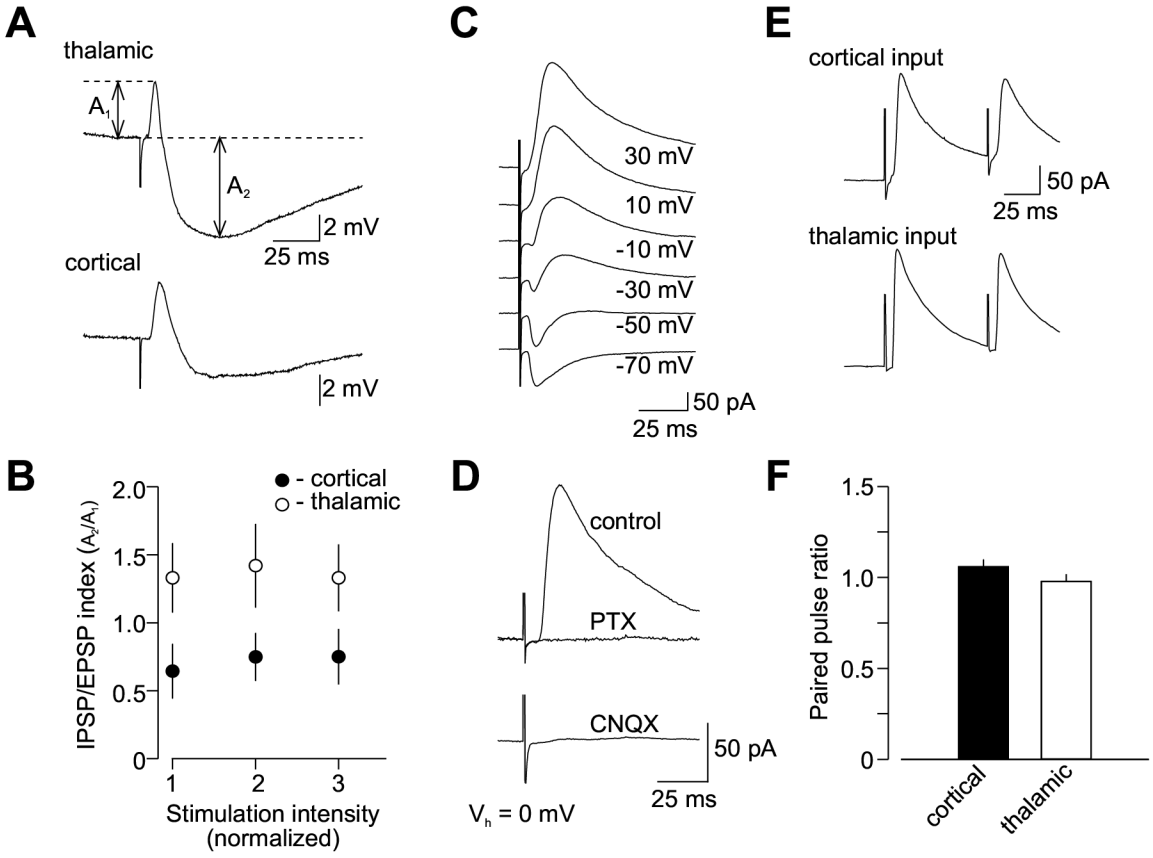

Figure 7.

Feed-Forward $GABA_A$ Receptor-Mediated Inhibition of Principal Neurons Is Stronger In Thalamic Input. (**A**) Examples of the EPSP/IPSP sequences recorded at a membrane potential of -55 mV in convergent cortical and thalamic pathways. Traces show average of 10 responses. (**B**) Input-output curves for the monosynaptic AMPAR EPSP and disynaptic $GABA_AR$ IPSP recorded at convergent cortical and thalamic pathways presented as an IPSP/EPSP index. The IPSP amplitude was normalized by the EPSP amplitude for both pathways in each individual experiment (n = 9). Feed-forward IPSP is enhanced in thalamic input compared to cortical input. The intensity of stimulation at both pathways was gradually increased from the threshold stimulus required to elicit IPSP, that was determined in each individual experiment, with an increment of 50 μA to produce synaptic responses of increasing amplitude. First points represent responses evoked by the stimuli at the threshold + 50 μA. (**C**) Biphasic synaptic currents recorded at holding potentials of -70 mV to +30 mV in cortical input. (**D**) Disynaptic $GABA_AR$ IPSCs recorded with the cesium-based intrapipette solution at a holding potential of 0mV. Under these conditions, the AMPAR EPSC did not make a detectable contribution to the evoked response, since it was blocked by PTX (50 μM). The IPSC was also blocked by CNQX (20 μM, lower trace) providing evidence of its disynaptic origin. (**E**) Examples of the $GABA_AR$ ISPC pairs induced in cortical input with a 70-ms interstimulus interval. Traces show average of 10 responses. (**F**) Summary plot of paired-pulse ratio (PPR) data for the IPSCs

recorded in cortical (n = 17) or thalamic (n = 15) inputs (mean ±SEM). PPR was calculated by dividing the second IPSC amplitude by the first IPSC amplitude

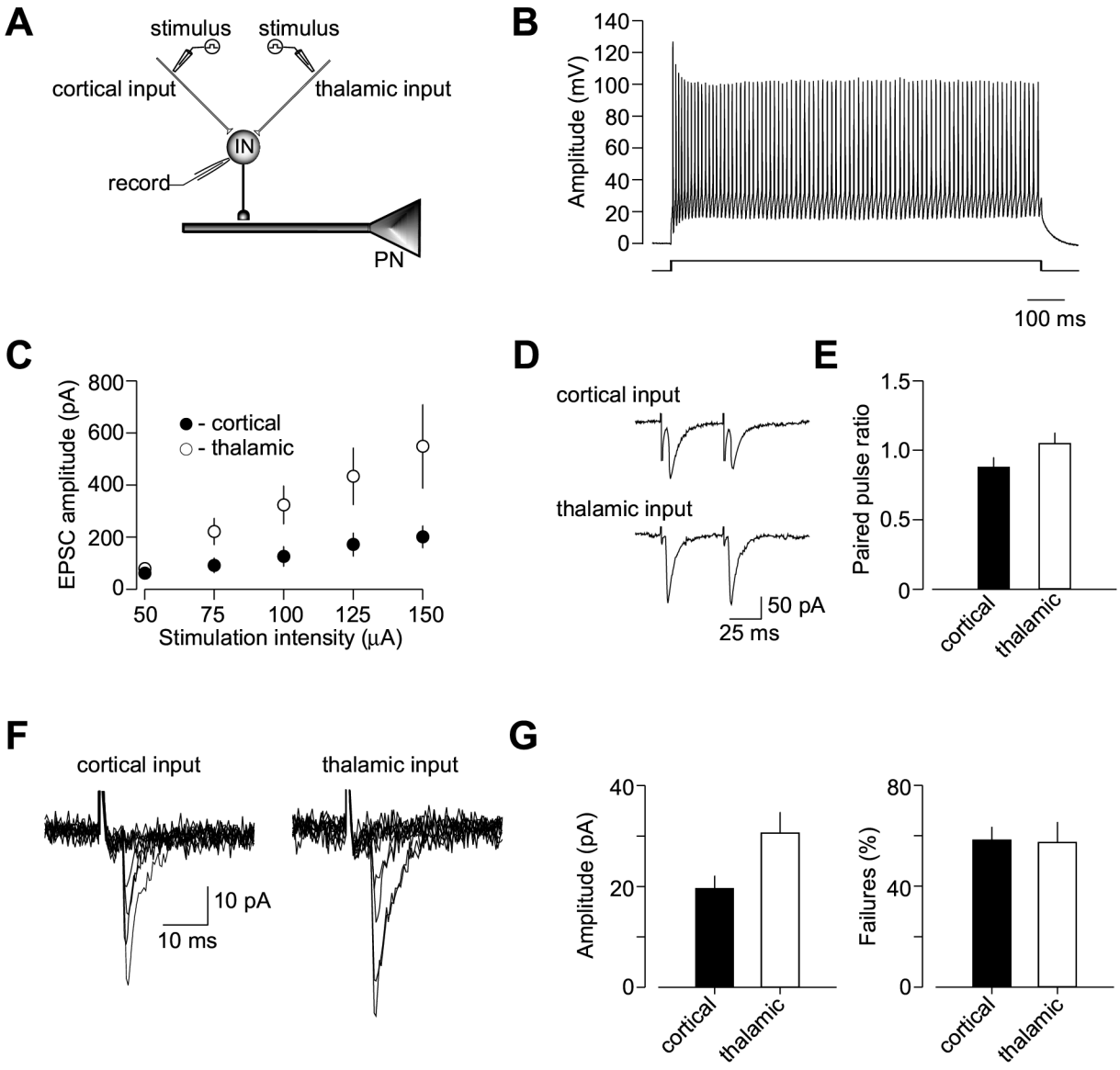

Figure 8.

Enhanced Excitatory Drive to Interneurons in Thalamic Pathway Mediates Input Specific Differences in Inhibition. (**A**) A schematic representation of the experimental design when cortical and thalamic inputs to the same interneuron were alternately activated. (**B**) The recorded cell was identified as interneuron based on non-accommodating firing pattern in response to prolonged depolarizing current injection. (**C**) Input-output curves for the AMPAR EPSC recorded in interneurons at a holding potential of -70 mV in the presence of PTX (50 μM) at convergent cortical and thalamic pathways (n = 5). A leftward shift in the input-output curves obtained in thalamic input, as compared to cortical pathway, indicates a stronger inhibitory drive in thalamic input. 10-15 EPSCs were recorded and averaged for each stimulation intensity. (**D**) Examples of the AMPAR EPSCs pairs induced with a 50-ms interstimulus interval in convergent cortical (top) and thalamic (bottom) inputs. Traces show

average of 10 responses. (**E**) Summary plot of paired-pulse ratio (PPR) data for the cortico-amygdala and thalamo-amygdala EPSCs recorded in cortical or thalamic inputs (n= 4, mean ±SEM). PPR was calculated by dividing the second EPSC amplitude by the first EPSC amplitude. (**F**) Superimposed traces of unitary EPSCs recorded in interneuron at -70 mV in response to stimulation of cortical (left) and thalamic (right) inputs. (**G**) Summary plot (mean ± SEM) of mean amplitude (left, n = 6) and failure rate (right, n = 6) estimates for unitary EPSCs in cortical and thalamic inputs to interneurons.

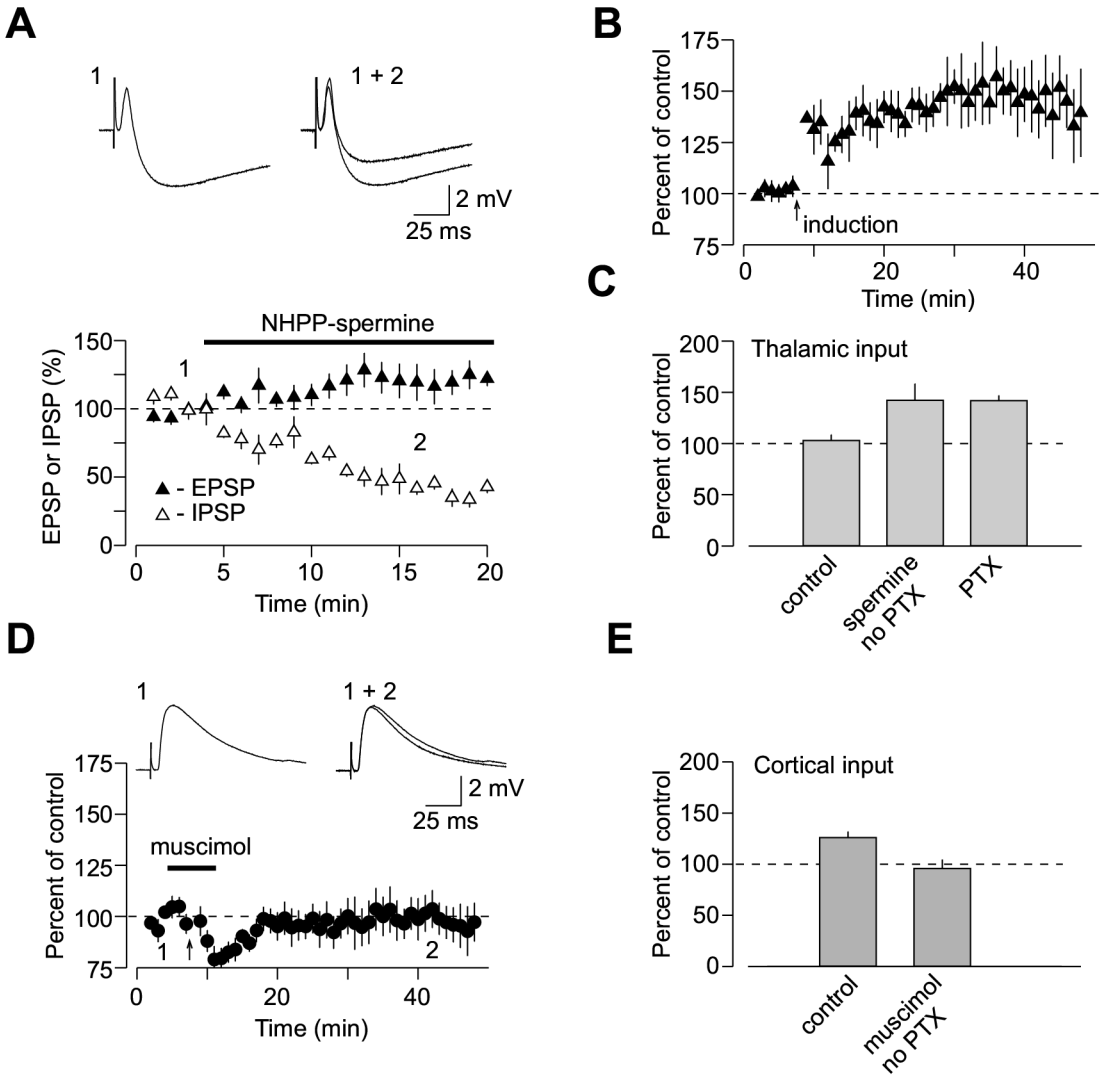

Figure 9.

Input Specific Differences in Inhibition Account for Spatial Specificity of LTP at Convergent Inputs in the LA. (**A**) Effects of NHPP-spermine on biphasic synaptic responses elicited by stimulation of thalamic input and recorded under current-clamp conditions in the LA neuron at -55 mV. NHPP-spermine (5 μM, n = 4) produced significant depression of feed-forward disynaptic IPSP (open symbols), with a little effect on monosynaptic EPSP (closed symbols). Graphs were obtained by normalizing data in 60 s epochs to the mean value of the baseline (pre-drug) responses (mean ±SEM). Insets show the averages of 8 biphasic responses recorded under baseline conditions (1) and during NHPP-spermine-induced depression (2). (**B**) LTP at thalamo-amygdala pathway induced in the presence of NHPP-spermine (5 μM) by the repetitive EPSP-AP paring using positive time intervals of +4 to +6 ms between the onset of the EPSP and the AP peak without PTX in the bath solution (n = 4). (**C**) Summary of LTP experiments. LTP in thalamic input was induced either without (control, n = 5) or with 100 μM PTX (n = 6; same data as in 1H) and in the presence of spermine (n = 4; mean ±SEM). (**D**) Induction of LTP at cortico-amygdala pathway by the repetitive EPSP-AP paring is

prevented in the presence of muscimol (2 μM). Insets show the averages of 8 responses recorded under baseline conditions (1) and after pairing (2). (**E**) Summary of LTP experiments in cortical input as in (D). LTP was induced either under control conditions (control: no PTX, n = 9; same data as in 1D) or in the presence of muscimol (n = 5; mean ±SEM).